The T-Taxol Conformation

Ana A. Alcaraz, Anil K. Mehta, Scott A. Johnson, and James P. Snyder*

Department of Chemistry, Emory University, Atlanta, Georgia 30322

Received November 7, 2005

T-Taxol is a proposal for the bioactive conformation of paclitaxel (PTX) derived from fitting ligand conformations to the electron crystallographic (EC) density. Although confirmed by a number of studies, some structural ambiguities based on the interpretation of two solid-state REDOR $^{13}C-^{19}F$ distances in a fluorinated PTX derivative remain. An evaluation of the static and dynamic properties of the PTX−tubulin complex shows that small 6−12° variations in calculated torsions and a justifiable increase of the REDOR distance error to $\geq \pm 0.7$ Å readily resolves key discrepancies around T-Taxol's service as the bioactive conformation. In addition, conformational analysis reveals a range of $^{13}C-^{19}F$ separations compatible with the REDOR measurements suggesting that the present PTX REDOR distances may not provide a precise model for bioactive, tubulin-bound bridged taxanes. In addition, we show that New York-Taxol (PTX-NY), a recently proposed alternative to T-Taxol, is incompatible with both the EC density and the activity of a highly active series of bridged taxanes.

Introduction

In the absence of a high-resolution structure, the determination of the conformation of a ligand at its binding site within a protein is an art. Between the extremes of well-defined models derived from X-ray structures of 2.0 Å or higher resolution and ill-defined models constructed from pharmacophores, electron crystallography (EC)[a] provides 3−4 Å resolution complexes. In this resolution niche, EC densities for the ligands are often incomplete and sensitive to the placement of nearby protein side chains. Interpreting the density in terms of ligand conformation depends both on model building and careful consideration of other external factors such as structure−activity relationships (SAR), photoaffinity labeling, and specific internuclear distances obtained from NMR analysis. The determination of the bioactive conformation of the breakthrough anticancer drug Taxol (PTX, **1**) in complex with β-tubulin is such a case.

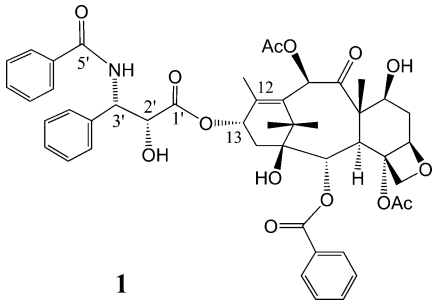

1

Although there is a rich history of synthesis and biological testing for PTX,[1] only after the compound was successfully introduced as a clinical drug[2] did a 3-D representation of the protein-bound entity become available. Nogales, Wolf, and Downing solved the EC structure of the α,β-tubulin dimer by analyzing polymeric sheets of microtubules stabilized by zinc cations and the bound drug.[3] Unfortunately, although the 3.7 Å resolution structure[4] presents the protein fold as a readily discernible collection of β-sheets and α-helices, it was insufficiently resolved to define the conformation of PTX. Consequently, the single-crystal X-ray structure of the related drug docetaxel (DTX, **2**)[5] was positioned in the ligand density as a placeholder.[3] This important but tantalizing result led to a number of efforts to define the details of ligand conformation, a factor important for further design and synthesis of improved anticancer agents. A number of groups synthesized bridged analogues based on various principles, but none of the early attempts proved to match PTX's profile against either the protein (in vitro) or the cells.[6,7] As discussed below, the T-Taxol conformer is unique in leading to the synthesis of bridged analogues that surpass the biological activity of PTX.

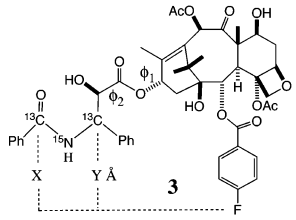

Conformer	r (X (F---C(O))	Y), Å (F---C-3')	deg ϕ_1	ϕ_2
REDOR[8]	9.8	10.3		
Polar[8]	10.4	9.6	-101	103
1JFF[11]	8.1	9.3	-94	56
T-Taxol[10]	9.1	9.9	-103	70
T-Taxol (i)	9.9	10.3	-89	70
T-Taxol (ii)	9.8	10.1	-103	82
T-Taxol (iii)	9.8	10.2	-97	76
PTX-NY[13]	9.4	10.0	-160	-100

Figure 1. $^{13}C-^{19}F$ REDOR distances (X and Y) for 2-(*p*-fluorobenzoyl)paclitaxel (**3**) compared with proposals for the β-tubulin-bound conformation of PTX (Å). Dihedral angles ϕ_1 and ϕ_2 correspond to the C12-C13-O-C1′ and O-C1′-C2′-C3′ torsion angles, respectively; for i-iii, see below.

The first structural analysis of tubulin-bound PTX came in the form of a collaborative solid-state NMR−REDOR study by the groups of Schaefer, Bane, and Kingston, who reported two distances between fluorine at the *para* position of the C-2 benzoyl group and the ^{13}C-labeled C-5′ amide carbonyl carbon (X, 9.8 Å) and the C-3′ methine carbon (Y, 10.3 Å) (Figure 1).[8] The uncertainties in both distances were estimated to be ± 0.5 Å.

This work interpreted the REDOR distances in terms of the hydrophobically collapsed polar conformer of PTX (Figures 1 and 2a).[9] However, the inactivity of a bridged analogue that enforces the same 3-D form fails to support it as the binding conformer.[6a] Subsequently, a model of the PTX−tubulin com-

* To whom correspondence should be addressed. Tel: 404-727-2415. Fax: 404-727-6586. E-mail: jsnyder@emory.edu.

[a] Abbreviations: PTX, paclitaxel; PTX-NY, paclitaxel-New York; DTX, docetaxel; NTX, nonataxel; 2FB-PT, 2-fluorobenzoyl paclitaxel; TB, tubulin; *t*-Bu, *tert*-butyl; EC, electron crystallographic; SAR, structure−activity relationship; REDOR, rotational echo double resonance; LMMC, low mode Monte Carlo; MD, molecular dynamics; ps, picoseconds; DMSO, dimethyl sulfoxide; D_{CF}, dipolar C−F coupling; MM3*, MMFF, MMFF94s, and AMBER, various molecular mechanics methods.

10.1021/jm051119r CCC: $33.50
Published on Web 03/24/2006

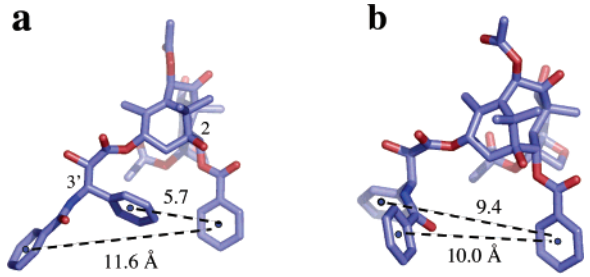

Figure 2. Two paclitaxel conformations displaying the distances between the centroids of the C2-benzoyl phenyl ring and the C3′ phenyl and benzamido phenyl rings (Å). (a) The polar conformation. (b) T-Taxol.

plex faithful to the EC density proposed another conformer, T-Taxol, which likewise conforms to the REDOR distance constraints.[10] Simultaneously and independently, a refinement of the EC tubulin−PTX structure (1JFF) at 3.5 Å resolution proposed a very similar ligand conformation.[11]

Two studies have since emerged that question the T-Taxol proposal on the grounds that the 1JFF structure does not meet the requirements of the REDOR data when interpreted strictly in terms of the ±0.5 Å error estimate (cf. Figure 1).[12,13] Both investigations mistakenly attribute 1JFF distances to the T-Taxol distances.[14] Interestingly, these reports point separately to the collapsed polar conformer and a modified T-Taxol conformer, respectively, derived from the same REDOR investigation as that from the better models, although both pairs of distances likewise fall outside the estimated error boundaries. The purpose of the present work is to critically examine the various proposals in light of the REDOR measurements to illuminate the limits of the NMR data and to re-affirm the suitability of the T-Taxol conformation as the bioactive form at the *β*-tubulin taxoid binding cleft.[13,15]

Variability of Unbound PTX Structures That Conform to REDOR Distances

There are many different PTX conformations that closely match the two intramolecular distances defined by the solid state NMR experiment. To examine the possible range of structures strictly meeting the REDOR measures, we have performed two low mode Monte Carlo conformational searches[16] for 2-(*p*-fluorobenzoyl)paclitaxel (**3**, Figure 1) using the MMFF and MM3* force fields and an aqueous continuum-solvation model.[17] Throughout the searches, the F−C-5′ and F−C-3′ distances were constrained to the REDOR values (9.8 and 10.3 Å, respectively). A total of 602 and 598 structures were obtained with MMFF and MM3*, respectively, within an energy window of 7 kcal/mol from the global minimum. The distance constraints were removed, and the two sets of conformations were fully optimized with the respective force fields. Forty-seven structures with MMFF retained the REDOR distances within ±0.3 Å, whereas 37 structures with MM3* did so.

Figure 3 displays a subset of the fully optimized conformations with retained REDOR distances for which the baccatin cores have been superimposed. As will be discussed in detail below, only two distances have been measured. As a result, the conformational profile of the system is not well defined. Within the boundaries of the search, the two phenyl groups emanating from C-3′ (Ph and NHCOPh) are free to occupy a wide range of locations. Consequently, although the NMR-determined distances provide important intramolecular measures for two C-13 side chain atoms buried within the volume of the paclitaxel molecule, they are silent with respect to the C-3′ terminal

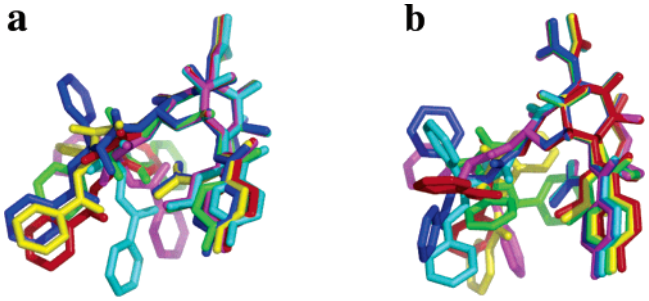

Figure 3. Spatial disposition of the *C*-3′ terminal phenyl groups (at the left side of both structures in a and b) resulting from two LMMC conformational analyses of the fluorinated PTX (**3**) C-13 side chain under conditions in which the F−C-5′ and F−C-3′ distances are within +0.3 Å of the REDOR values of 9.8 and 10.3 Å, respectively. (a) MMFF force field. (b) MM3* force field.

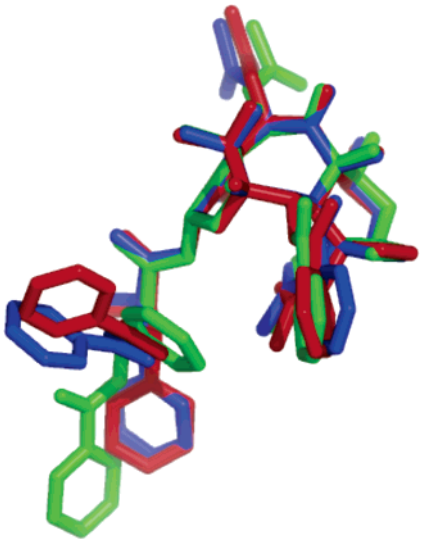

Figure 4. Spatial disposition of the *C*-3′ terminal phenyl groups from superimposing the baccatin cores of T-Taxol (blue), 1JFF (red), and the polar conformation (green).

hydrophobic contacts between the ligand and the protein. As a result, the REDOR outcome cannot distinguish between the T-Taxol and polar conformations (Figure 1).

A subtler question concerns the spatial variability of the same two rings when the empirical structures for the bound conformation are superimposed. Figure 4 depicts the situations for T-Taxol,[10] 1JFF,[11] and the polar conformation when the C-2, C-4, C-13, and C-15 baccatin core atoms are matched.[18] Clearly, the first two T-type structures present a fundamentally different orientation of the C-3′ phenyl rings compared with that of the polar conformation. At the same time, none of the structures adhere strictly to the 9.3−10.3 and 9.8−10.8 Å ranges dictated by the ±0.5 Å error boundaries derived from the REDOR data, although the polar and T-Taxol forms come within 0.6/0.7 and 0.7/0.4 Å, respectively. The large 1JFF differential of 0.5−1.7 Å is undoubtedly a consequence of the low-resolution data (3.5 Å) achieved during refinement.

T-Taxol and the C-13 Side Chain Dihedral Angles

Concerning T-Taxol itself, what are the origins of the observation that the F−^{13}C distances from the computationally refined structure fall near the lower boundaries of the error bars? This can be traced to small deviations in the C12−C13−O−C1′ and O−C1′−C2′−C3′ dihedral angles (*ϕ*) compared to those required for exactly meeting the REDOR constraints. In the published T-Taxol structure,[10] these are −103 and 70°, respec-

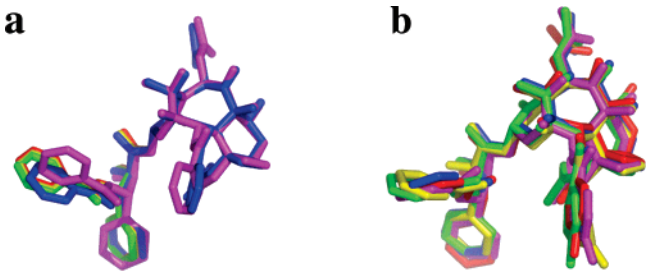

Figure 5. Spatial disposition of the *C*-3′ terminal phenyl groups from superimposing the baccatin cores of various T-Taxol forms. (a) T-Taxol[10] (blue), 1JFF PTX[11] (magenta), and the torsion angle variants (i)−(iii) (red, green, and yellow) from Figure 1. (b) Snapshots from the MD trajectory of F-substituted T-Taxol (**3**) docked in β-tubulin.

tively. A separate reduction of the first dihedral angle by 14 to −89° or an enlargement of the second by 12 to 82° provides perfect agreement with the REDOR distances (T-Taxol (i) and (ii), respectively, in Figure 1). If both angles are simultaneously altered to −97° and 76°, respectively, a diminutive 6° change for each, the structure is once again brought into perfect alignment with the solid-state distances (T-Taxol (iii), Figure 1). One possible interpretation of the distance discrepancies, then, is that the Kollman all-atom AMBER force field[19] used in the PTX−tubulin structure refinement utilized torsional parameters for the two angles in question that were not fully optimized. Nonetheless, the small 6−14° ϕ-angle variations do not alter the fundamental nature of the T-Taxol conformation. The differences are readily accommodated by the realization that small torsional angle variations correspond to ambient vibration about the corresponding energy minima. Figure 5a depicts the spatial consequences for the C-3′ phenyl rings across the range of angles with $\Delta\phi = 6-14°$. Even the somewhat deviant 1JFF PTX structure appears to be a closely related member of the T-taxoid family. The next section examines this perspective from the viewpoint of molecular dynamics (MD).

Molecular Dynamics of T-Taxol in β-Tubulin

The analysis presented in the previous section examined individual static PTX structures to determine their viability as T-Taxol representatives. In a second study, we adopted a dynamic approach to learn how thermal motion at room temperature might alter the F−C separations when PTX is bound to β-tubulin. Because His227 is believed to be in intimate association with the bound drug, we treated the imidazole ring in both its neutral and protonated states. The corresponding PTX−tubulin complexes were subjected to molecular dynamics for 5 ps at 300 K with the Tripos force field,[20] during which time the F−C-5′ and F−C-3′ separations were constantly monitored. For neutral His227, the F−C distances fell in the 8.3−9.8 and 8.7−10.3 Å ranges, respectively. For the protonated side chain, the values oscillated more broadly between 6.8 and 10.2 and 7.5−10.2 Å. The Tripos force field, like AMBER, delivers values at the low end of the 268 K REDOR error boundaries. To illustrate the relationship with the static T-forms depicted in Figure 5a, the corresponding view for snapshots of **3** across the His-neutral trajectory are shown in Figure 5b. Qualitatively, the conformational fluctuations are very similar.

Apart from the actual numerical values of REDOR-determined distances, the present case is an illustration of the important fact that molecular structures above absolute zero are not static entities. Whether internal or external to a protein, small molecules are in constant motion, oscillating around the values measured by structural analyses. The degree to which they experience motion is related to both the temperature and the medium employed for the measurements. An illustrative study in this respect examined a DMSO solvate of 10-deacetylbaccatin III by ^{13}C NMR in the solid state.[21] Varying the temperature from 23 to −120 °C resulted in a strong chemical-shift dependence for the aromatic ring carbons of the C-2 benzoyl group. The changes were interpreted as a result of the molecular motion causing the conjugated C═O and the phenyl groups to significantly deviate from planarity. The baccatin III work[21] suggests that the movement within the C-2 center of **3**, which contains the fluorine label, may be significant. This is of interest because the molecular motions of labeled atoms can reduce dipolar interactions resulting in apparent overestimation of internuclear distances.[22]

Limits on the REDOR Experiment

The Schaefer group's double REDOR solid-state NMR measurement of F−^{13}C distances for quadruply labeled **3** (Figure 1), bound to tubulin that was polymerized in vitro, encompassed 8 million scans and required three months of acquisition time. The experiment involved continuous dephasing by ^{15}N (^{13}C-{^{15}N}) and ^{19}F (^{13}C{^{19}F}) to generate difference spectra S_0 and ΔS, respectively. The $\Delta S/S_0$ ratio measures the dipolar coupling between the ^{13}C and ^{19}F atoms. Because the ratio depends only on the ^{13}C−^{19}F distance (r_{CF}), acquisition of the internuclear separations only requires the determination of the $\Delta S/S_0$ value at a single dephasing time.

In the REDOR analysis of **3**, the consideration of signal-to-noise in the $\Delta S/S_0$ ratio led to the estimate of a 6% uncertainty in the F−^{13}C distances, that is, ±0.5 Å.[8] Despite the enormous resources expended to generate the distances, there are inherent limitations associated with fitting a single-parameter curve to a single data point, the latter being a necessity in the analysis of Schaefer et al. because each additional point would require at least three additional months of machine time. As a result, we have reexamined the error calculations and certain assumptions underlying the REDOR measurements.

REDOR Error Recalculation. The dipolar coupling (D_{CF}), hence the $\Delta S/S_0$ ratio, between two NMR active nuclei is inversely proportional to the cube of the internuclear distance (r_{CF}) between them; $D_{CF} \approx 1/r^3$. Using standard error analysis for the 9.8 Å distance, the reported value of $\Delta S/S_0$ (0.14), and the 20% reported error, the error recalculation is as follows

$$\pm\frac{r}{r_{CF}} = \pm\frac{\frac{1}{3}(0.2)(\Delta S/S_0)}{\Delta S/S_0} = \pm\frac{\frac{1}{3}(0.2)(0.14)}{0.14} = \pm 6.7\%$$

where $\pm r$ is the error in the calculated internuclear distance. Calculating the error in a similar manner for the 10.3 Å distance translates into 9.8 ± 0.7 Å and 10.3 ± 0.7 Å, providing a slightly expanded error window by comparison with that estimated previously. In this context, the REDOR measurement accommodates the structures previously published for both the polar conformation and T-Taxol (Figure 1).

The REDOR dephasing curves corresponding to the reported distances[8] and the recalculated ±0.7 Å error are displayed in Figure 6. Although the measured ratios accurately fall on the theoretical curves represented by the solid lines, a critical element inherent in the determined ^{13}C−^{19}F distances is that the distance measurement relies on fitting a single-parameter curve to a single data point. Although the ±0.7 Å bracket represents the experimental error, there are a number of reasons for believing that even this range of ^{13}C−^{19}F distances may be overly restrictive. The basis for this assertion follows.

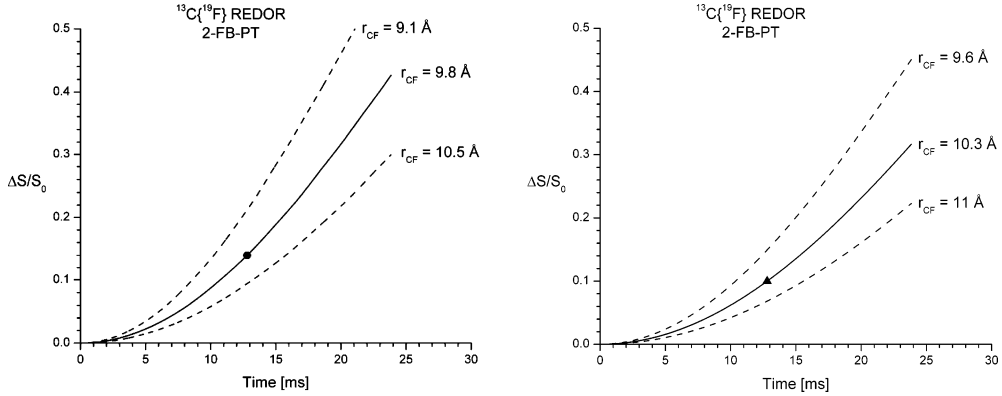

Figure 6. Experimental dephasing (from ref 8) for ^{13}C-5′−^{19}F (●) and ^{13}C-3′−^{19}F (▲) and the calculated REDOR curves assuming a single ^{13}C−^{19}F distance to each ^{13}C center. The solid lines correspond to the ^{13}C−^{19}F distances[8] and the dotted lines represent the ±0.7 Å error.

Conformer Distributions of 3. The REDOR curves are calculated assuming a single ^{13}C−^{19}F distance and the lack of significant molecular motion. However, the potential conformer distribution of the *C*-3′ terminal phenyl groups implied by the MD simulations and the solid-state baccatin III ^{13}C spectra[21] is consistent with the view that **3** experiences dynamic conformational equilibration in the solid state. An alternative viewpoint arises from the observation that in the REDOR experiment the tubulin-microtubule samples stabilized by the labeled 2-flurobenzoyl PTX (2-FB-PT) were rapidly frozen in liquid nitrogen (77 K) and lyophilized for 3−4 days.[8] It has been argued that such freeze drying traps all conformations present in the solution prior to flash freezing and thereby leads to microheterogeneity accompanied by the lack of equilibration.[23] However, raising the temperature from 77 to 268 K (−5 °C), where the REDOR experiment was conducted, can potentially reestablish interconversion among a distribution of forms.[21,24,25] Accordingly, the C-2 and C-13 side chains furnishing the distance measurements may well oscillate around a cluster of interconverting structures characterized by both high-amplitude torsional vibrations and interconverting conformations. As a result, the distributions depicted by the MD simulations may contribute to the observed REDOR dephasing.

In principle, REDOR can disentangle conformational effects in the solid lyophilized sample. However, to deconvolute internuclear distances for a possible range of trapped conformations, several dephasing times need to be collected. Multiple data points are required because dephasing for a distribution of distances depends on two parameters, namely, the mean (or average) distance and the distribution.[26] In an attempt to estimate the effect of C-2 and C-3′ side-chain distributions on the shape of the REDOR dephasing lines in the absence of multiple measurements, we have modeled the dependence of the $\Delta S/S_0$ ratio in terms of Gaussian half-widths (Figure 7; Table 1; see Methods). For the 9.8 and 10.3 Å ^{13}C−^{19}F distances, Gaussian distributions of 0.8 and 1.6 Å give results essentially identical to that for no distribution. As there is only a single REDOR data point, all three models (no distribution, 0.8, and 1.6 Å distributions) are consistent with the distance data.

The Gaussian curves are properly interpreted as the distribution of conformations observed in the solid state with different ^{13}C−^{19}F separations. The larger the full-width half-maximum of the Gaussian distribution, the larger the disorder. The result of fitting the data to a distribution suggests that the ^{13}C−^{19}F distances would increase, at most, by 0.1 Å (Table 1, see Methods). However, for these distributions and distances, the raw distance error estimate is the same, ±0.7 Å. For reasons

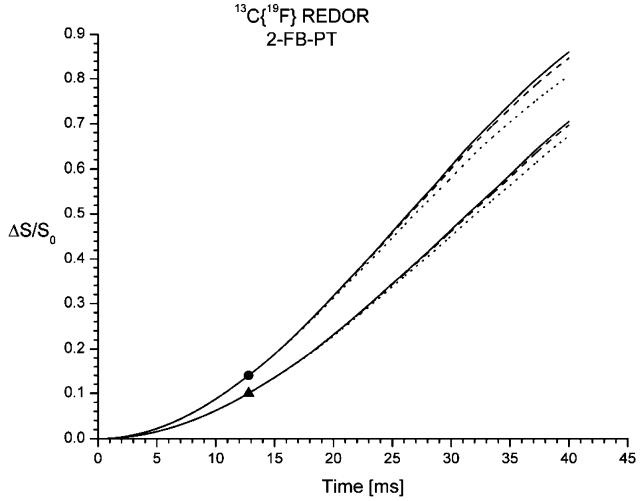

Figure 7. REDOR plots of ^{13}C-5′−^{19}F (●) and ^{13}C-3′−^{19}F (▲) dephasing with calculated curves for no distribution (—) and Gaussian distributions with full-width and half-maximum widths of 0.8 Å (....) and 1.6 Å (---). Distances from ref 8.

Table 1. Full-Width at Half-Maximum of Calculated Gaussian Distribution as a Function of ^{13}C−^{19}F

	width of Gaussian distribution (Å)	distance (r_{CF}) (Å)
carbonyl	0	9.8
	0.8	9.8
	1.6	9.9
methine	0	10.3
	0.8	10.4
	1.6	10.5

expressed above, this analysis is also consistent with the view that a ±0.7 Å error of the distance measurement resulting from fitting a single-parameter curve to a single data point is overly conservative.

Lyophilization of the TB−Ligand Complex. Another potential source of difference between the solid state and EC-refined distances arises from the 3−4 day lyophilization to which the tubulin-**3** NMR samples were subjected. The purpose of the process is to remove sufficient water to produce a solid but leave one or two aqueous solvation shells around the protein intact. In addition, to protect the surface of the protein in the absence of bulk water, lyophilization is performed in the presence of a stabilization matrix. In the case of the tubulin−2-(*p*-fluorobenzoyl) PTX complex, polyvinyl pyrrolydine was employed. Following the dehydration treatment, the presence

of intact microtubules was detected in the reconstituted lyophilized sample by electron microscopy.

Despite these precautions and controls, the actual number of water layers remaining after lyophilizaton is unknown. Likewise, the nature and extent of water structure near regions of relative hydrophobicity, for example, near the taxoid hydrophobic cleft, is undefined. Given that PTX is believed to bind either at the inner[3,27] or at the outer[28] surface of the microtubule, one face of the molecule is exposed to the aqueous environment, whereas the other concave nonpolar one may share the binding pocket with a small number of water molecules.[29,30] Consequently, any disruption or reorganization of the first solvation shell could have an effect on how deep the ligand sits in the pocket, on features of conformation, or on ligand mobility.

Two interesting studies in this respect focus on a short peptide and a protein. The first evaluated the solid-state ^{13}C and ^{15}N NMR spectra of crystalline pentapeptide Leu- and Met-enkephalins experiencing different degrees of hydration.[25] Not only are the peptides' backbones and side chains dynamic in the 0 to −100 °C temperature range, but the conformational disposition is influenced by dehydration. Significantly, REDOR distances were shown to change by as much as 25% as a result of partial dehydration. Although the hydrated crystalline enkephalin system is not a mimic of the TB−PTX complex in the solid state, the work nonetheless teaches that the modification of the solvation shells near the binding site carries the potential for the alteration of both the static and dynamic structural features of the ligand. To evaluate motion in hydrated protein microcrystals, the second investigation compared the X-ray crystal structure and solution NMR analysis of ubiquitin with solid-state NMR measurements of the same protein labeled uniformly with ^{13}C and ^{15}N nuclei.[31] Reduced dipolar couplings were observed for residues with increased backbone motion, as measured both by solution-state NMR and increased crystallographic B factors. The three measurements concur that sectors of hydrated proteins near room temperature (10 °C) experience significant motion. In summary, both the enkephalin and ubiquitin results provide an additional reason for not expecting perfect agreement between REDOR- and EC-determined internuclear distances.

We do not propose that uncertainties in the solvation properties of the protein binding pocket in any way invalidate the REDOR measurements. We do suggest, however, that the error estimates of ±0.5 and ±0.7 Å are too narrow by this standard. Consideration of fitting the REDOR curve to a single point, conformer distribution, molecular motion, and variations in the nature of binding-site hydration relative to soluble or polymerized protein can easily explain the minor discrepancies between REDOR- and EC-determined intramolecular F−C distances. In summary, the ^{13}C−F REDOR distances are fully supportive of the T-Taxol and PTX-NY binding conformations as they are of the polar and numerous other energy minimum conformations. A critical question is whether these conformers are also consistent with the biophysical properties of other taxane analogues. Accordingly, the bioactivity of docetaxel (DTX), nonataxel (NTX), and a set of bridged taxanes is discussed below.

Docetaxel and Nonataxel

Docetaxel (DTX, **2**) is a clinically effective anticancer agent that is twice as effective as PTX at stabilizing microtubules and killing murine P388 leukemic cells.[32] Nonataxel (NTX, **4**) is a nonaromatic taxane derivative that is 2−7-fold more cytotoxic than PTX in a number of cell lines.[33] Both DTX and NTX differ structurally from PTX in replacing the benzamido side chain phenyl with the *O*-*tert*-butyl moiety. In addition, NTX employs isobutenyl instead of the phenyl functionality at C-2 and C-3′.

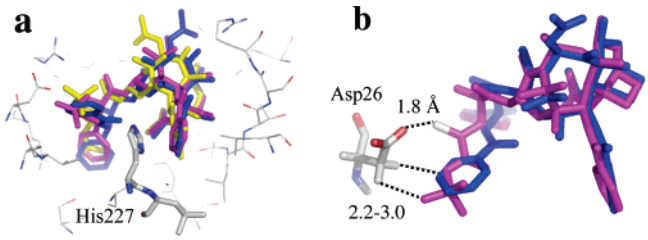

Figure 8. (a) Superposition of PTX (blue), DTX (magenta), and NTX (yellow) in the T-Taxol−tubulin binding site showing tubulin's His227 sandwiched between the C-2 phenyl and C-3′ substituents. (b) The spatial relationship of PTX and DTX with Asp26. Both C-3′ side chains experience van der Waals contact with the residue; H−H distances range from 2.2 to 3.0 Å. DTX makes a productive NH−O hydrogen bond with the carboxylate (1.8 Å), whereas PTX does not (4.2 Å).

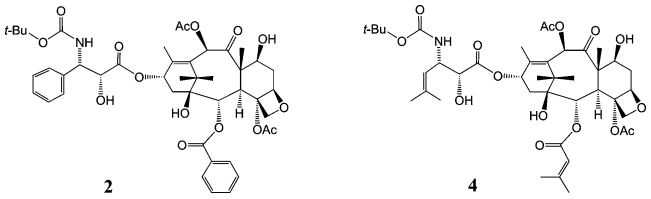

Given the different steric requirements for the hydrophobic termini at C-2 and C-3′ for **1**, **2**, and **4**, we decided to examine the relative disposition of the analogues in the binding site associated with T-Taxol (Figures 2b, 4, and 5). The latter two structures were modified from the T-form of PTX and docked into tubulin by superimposing the baccatin cores. Each model was subjected to cold MD (20 K) with the backbone held in a fixed position to remove short ligand−protein contacts and optimized with the Tripos force field (Methods).[20] Figure 8a illustrates the overlap of the three structures in the T-conformation within the tubulin taxane binding pocket. Each structure resides comfortably in the site and shows no evidences of high-energy contacts with the protein.[34] However, Figure 8b, depicting the overlapped NH−C(═O)-R moieties for **1** and **2**, shows that both the phenyl and *O*-*t*-Bu groups, respectively, are in van der Waals contact with the CH_2 of the Asp26 side chain. The geometry around the carbamate oxygen atoms in both DTX and NTX positions the amide groups to permit a hydrogen bond between one of the Asp carboxylate oxygens and NH (1.8 Å). However, the shorter connector and the less flexible C-3′ benzamido group for Taxol leads to an AspCOO−HN distance of 4.2 Å, short enough to sustain a productive electrostatic interaction but too long to qualify as a hydrogen bond. The more favorable interaction could well be the source of the 2−7-fold increase in activity in DTX and NTX in comparison with that in PTX.

A related analysis in a Taxol-resistant epidermoid tumor line with the acquired Asp26Glu mutation likewise employs the T-Taxol model to explain the PTX versus DTX-resistance profile in the resistant cells.[35] Again, the DTX NH has been proposed to form a strong hydrogen bond with the Glu carboxylate, whereas PTX is prevented from doing so by steric congestion.

Bridged Taxanes

Four research teams have prepared a wide range of bridged PTX analogues based on several conformational themes in an attempt to lock the molecules into the actual binding conforma-

tion.[6,7] The only design approach that has been able to match and surpass the biological action of parent PTX **1** in both cytotoxicity and in vitro microtubule assembly assays is that based on the T-Taxol conformation.[7,36] In this conformer, a short separation of 3−4 Å between the methyl of the C-4 OAc and the ortho position of the C-3′ phenyl suggested that short bridges between these centers would constrain the molecule largely to the T-taxane shape. A generic representation of the bridged series is given by **5**, whereas **6** (C-2 *para*-X = H) exemplifies a structure with at least a 20-fold greater potency than PTX in the A2780 ovarian cancer cell line and a 2-fold greater effect in the microtubule assembly assay.[36]

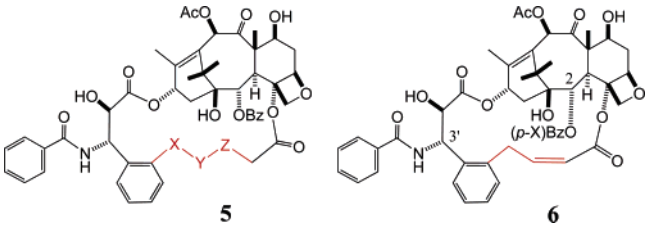

Conformational analysis of **6** (C-2 *para*-X = H), employing the MMFF94s force field,[37] yielded 93 conformers, 12 of which fall into the T-family by the measure of the distances between the centroids of the C-2 and C-3′ phenyl rings (Methods, Conformational Searches). The C-2 benzoyl phenyl was supplemented with a *p*-F atom, and the F−C-3′ and F−C-5′ distances that were measured ranged from 8.8 to 9.8 and 7.4 to 10.0 Å, respectively. These values average to approximately 1 Å lower than the REDOR distances. A more specific measure for the T-form is the distance between centroids of the C-2 benzoyl phenyl ring and the C-3′ phenyl and C-3′ benzamido phenyl rings. Unlike the C-3′ and C-5′ centers with the potential to relocate within the van der Waals surface boundaries of the bound taxane ligand, these three rings are in direct contact with the protein amino acid side chains composing the binding pocket. Not a single example of the New York conformer, PTX-NY (see below), was found among the 93 conformers of **6**.

As mentioned above in connection with Figure 3, the REDOR distances tolerate a wide variation in the positions of the two terminal *C*-3′ phenyl groups. The reverse situation appears to be mutual. Namely, the terminal phenyl rings in taxane derivatives can be located in T-form locations although permitting a range of C−F distances. Four of the *p*-fluorinated C-2 phenyl conformers of **6** (C-2 *para*-X = F) were docked into β-tubulin and, although displaying shorter C−F separations within the van der Waals volume of the molecule, they nonetheless sustain phenyl centroid−centroid distances very similar to that of T-Taxol (9.4 ± 0.1 and 10.0 ± 0.3).[10] Figure 9 illustrates one of the four conformations in the tubulin−taxane pocket following an extensive MD treatment (see Methods) superimposed on the EC structure of PTX[10] in the same pocket. This highly active and constrained T-taxoid paclitaxel analogue (**6**) (C-2 *para*-X = F) does not appear to place its C-3′ phenyl rings precisely in the same locations as those of PTX. The rather broad hydrophobic cleft is tolerant of small phenyl displacements along this wall as suggested by the molecular dynamics portrait in Figure 5b and the lack of significant side-chain displacement from PTX to **6** (C-2 *para*-X = F) (Figure 9). The same does not appear to be true along the floor of the pocket when a longer bridge falls outside the parent Taxol molecular volume.[38]

In support of these ideas, a very recent report by Dubois and co-workers implemented a taxoid design based on bridging

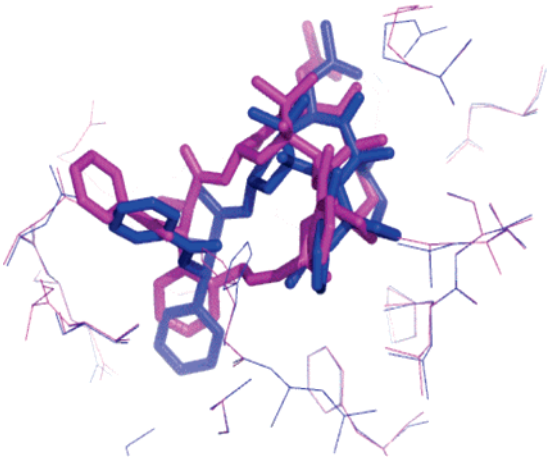

Figure 9. T-taxoid conformation of C-4 to C-3′ bridged taxane **6** (C-2 *para*-X = F) docked in the β-tubulin taxane binding site (magenta). The EC structure of PTX is shown in blue. The surrounding side chains show little change between the structures.

between the C-2 benzoyl phenyl group and an alkyl replacement of the C-3′ benzamido moiety.[39] The tubulin polymerization assay ranked one compound to be as effective as PTX, although the compound fell considerably short of PTX in the cytotoxicity assays. The authors interpreted the results as confirmation of the T-conformer.

An alternative interpretation of the binding conformation of PTX has been forwarded by Ojima and co-workers[13] on the basis of the observation that a photoactive C-7 benzodihydrocinnamyl derivative of PTX labeled the M-loop of β-tubulin exclusively at Arg282.[40] A Monte Carlo conformational analysis of the covalent protein−label complex delivered a number of conformers. The one that best matched the REDOR−NMR data (PTX-NY, X = 9.4, Y = 10.0 Å, Figure 1) was selected as the tubulin-bound PTX conformation.[41] In the spirit of the T-Taxol design study,[36] short distances were measured between the C-4 acetyl methyl and the C-2′ carbon and between the C-14 center and the C-3′ benzamido phenyl. The analysis led reasonably to the design of structures **7** and **8** (SB-T-2053), respectively, which bridge the model's contiguous centers. The compounds were prepared and tested against a variety of cell lines and subjected to the microtubule stabilization assay.

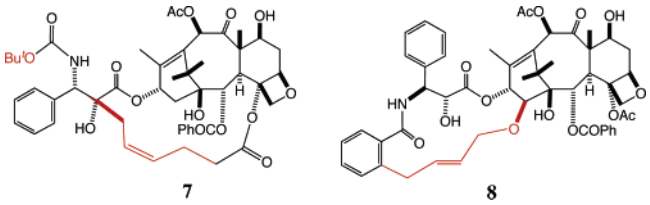

Compound **7** with a bridging point from C-4 OAc similar to that in **5**−**6** proved to be completely inactive. In contrast, C-14 to C-3′ analogue **8** was shown to be as effective as PTX in inhibiting tubulin depolymerization, although in several breast and colon cancer cell lines it is 4−20-fold less cytotoxic than the parent drug.

The study by Ojima and co-workers rejects the T-Taxol conformer on the basis that 1JFF-PTX does not conform to the REDOR distances.[11,13] However, as pointed out in Figure 1 and implied by the subsequent discussion, the T-Taxol form and the PTX-NY models appear to be very similar but both differing somewhat from 1JFF PTX. In an effort to analyze the New York construct, we performed a 5000 step low mode Monte Carlo conformational search for the 15-membered ring of **8** that

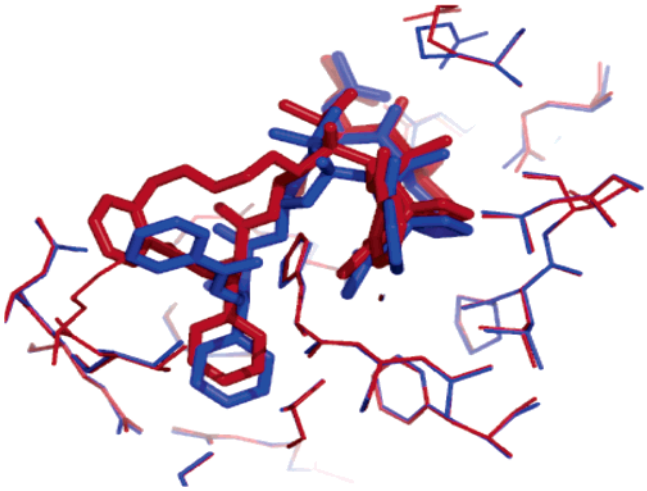

Figure 10. Superposition of β-tubulins from the optimized protein−ligand complexes containing T-Taxol (blue) and bridged **8** (red). The active-site side chains (blue/red) show little change, whereas **8** is seated a little higher than T-Taxol in the binding pocket.

encompasses both the C-13 side chain and the C-14 to C-3′ benzamido bridge. The resulting conformational pool contains 105 structures, 28 of which sustain the T-Taxol geometry. One of these was docked into the taxane site of β-tubulin and subjected to a series of molecular dynamics steps at 20 K to remove unfavorable steric contacts (Methods). The simulation was continued at 350 K for 5 ps to model the behavior of compound **8** in the protein.

As is evident from Figure 10, the side chains of the protein around the binding pocket, colored red and blue, change very little. Compound **8** is almost identically seated to T-Taxol with the exception that the linker relocates the C-3′ benzamide group somewhat less deep in the pocket. And as observed for bridged **6**, the C-3′ phenyl rings are shifted somewhat from those of PTX. Nonetheless, **8** displays distances between the centroid of the C2-benzoyl phenyl and the C-13 terminal phenyls, very similar to those found for T-Taxol in the EC-refined model (C-3′ benzamido Ph: 10.0 vs 9.4 Å; C-3′ Ph: 9.6 vs 10.0 Å).[10] A characteristic feature of the complex is that the C-2′ OH group is associated with the backbone NH of Gly368 as it is in the EC model. This contrasts with a proposed reorientation[13] of the OH functionality in PTX-NY (see below). More recently, the Ojima group has prepared a truncated C-4 to C-3′ taxane and argued that this represents another example of the PTX-NY conformation.[42] Re-analysis illustrates that this structure is likewise readily accommodated by the T-Taxol geometry.[43] Clearly, the distribution of forms represented by the structures in Figure 5b is accessible to bridged taxanes with very similar but nonidentical spatial requirements.

New York Conformation and the Electron Crystallographic (EC) Density

The recent paper by Ojima and colleagues, proposing a conformationally modified C-13 T-Taxol structure as the bioactive form (PTX-NY),[13b] comments that the low resolution of the tubulin−PTX complex density map eliminates the possibility for distinguishing between T-Taxol and the New York variation. It is accurate to state that during the initial structure-building process, the EC density alone was not sufficient to provide an unambiguous solution to the PTX binding problem.[3] The follow-up refinement that delivered 1JFF came close,[11] whereas modeling and NMR combined with the EC density yielded a well-defined structure with predictive

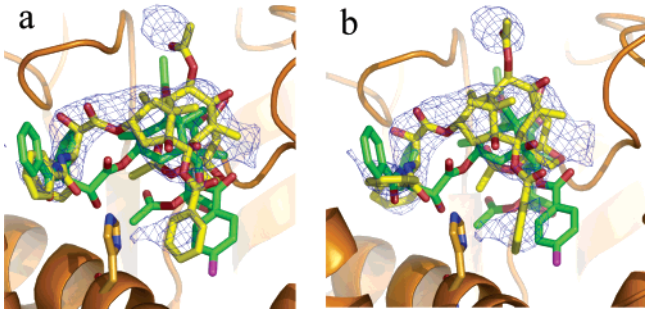

Figure 11. The structures of tubulin-bound Taxol (yellow) and 2-FB-PTX-NY (green) superimposed in the β-tubulin binding site. (a) The T-Taxol[10,45] $2F_{obs}-F_{calc}$ density map is shown as a blue 3-D contour. (b) The 1JFF Taxol[11] $2F_{obs}-F_{calc}$ density map is likewise shown as a blue 3-D contour.

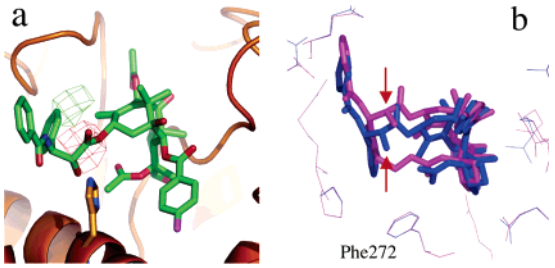

Figure 12. (a) Difference maps ($F_{obs}-F_{calc}$) for the 2-FB-PTX-NY structure. Green corresponds to unfilled density and red corresponds to incorrectly filled density. (b) PTX-NY in Figure 11 (blue) supplemented by a CH_2-CH_2 tether as in **5** (X = Y = Z = CH_2; magenta) followed by MD in the tubulin binding site. Red arrows indicate the movement of the C-2′ OH of the bridged analogue, a structure displaced from the binding site by a clash of the bridge with Phe272.

power.[10,36] Although the density in question is incomplete and weak in regions (e.g., between C-2 and the terminal benzoyl phenyl),[10] it is strong and discriminatory with respect to the conformation of the C-13 side chain. Figure 11, comparing T-Taxol and 1JFF Taxol against the New York conformer constructed from published torsion angles,[13b] is illustrative.

Figure 11a depicts the T-Taxol and the PTX-NY structures superimposed in the tubulin binding site simultaneously displayed with the $2F_{obs}-F_{calc}$ omit map[44] for the ligand. The strong EC density displayed as a blue grid along the C-13 side chain from C-1′ to C-3′ illustrates that T-Taxol (yellow) perfectly matches the experimental data. In contrast, the conformationally inverted C-2′ center in PTX-NY (green) falls well outside the density.[45] A comparison of the New York conformer with the PTX structure derived from the EC-refined complex 1JFF delivers the same result (Figure 11b). As emphasized above, although T-Taxol and the 1JFF variation sustain somewhat different C-13 torsions and internal distances (Figure 1), the structures fundamentally occupy the same space in the β-tubulin taxane binding pocket. A third test of the New York conformation's ability to fit the density was carried out by performing low-temperature molecular dynamics on the tubulin−PTX-NY complex using the structure depicted in Figure 11 (green, PTX). Slight movements of the ligand in the pocket were observed, but it essentially retained the same conformation and binding-pocket orientation. The corresponding $2F_{obs}-F_{calc}$ omit map is qualitatively and quantitatively similar to that pictured in Figure 11 (Supporting Information).

To examine this point further, Figure 12a presents the difference maps[44] ($F_{obs}-F_{calc}$) for PTX-NY, as depicted in Figure 11. Where model atoms lie outside the $2F_{obs}-F_{calc}$ contours, the $F_{obs}-F_{calc}$ map portrays them within the negative

(i.e., red) contours. Positive (i.e., green) contours highlight the correct locations for the same atoms. Thus, the green region represents the experimental density that is unfilled by the model structure, whereas the red grid corresponds to a spatial location that is improperly filled with the C-13 side chain. A similar exercise for the molecular dynamics relaxed form of the tubulin−New York PTX complex yielded the same result (Supporting Information). Taken together, the maps clearly distinguish the two conformations and affirm that T-Taxol is the conformer that best fits the EC density.

Finally, as mentioned above, the T-Taxol conformer has been used to design highly active taxane analogues with short bridges as a result of H−H distances measured at 2.5−2.9 Å between the C-4 acetate methyl group and the ortho position of the C-3′ phenyl. For example, compound **5** (X−Y−Z = CH_2-CH_2), incorporating a two carbon tether between these centers, is 2−13-fold more cytotoxic than PTX depending on cell line and 5-fold as effective in the tubulin aggregation assay.[36] Is the New York proposal predictive of this taxane modification? The corresponding H−H separations in the MD-optimized structure described in the previous paragraph were measured to be 3.5−5.3 Å. Although these quantities might possibly motivate bridging between the two centers in question, an inspection of PTX-NY reveals that the location of the C-2′ OH group would interfere with such a bridge. To test this idea, we converted the New York conformer shown in Figure 11 into **5** (X−Y−Z = CH_2-CH_2) and performed low-temperature MD followed by MMFFs optimization in the tubulin binding site. Whereas protein-free optimization of the bridged species caused a major conformational reorganization,[45] the rather tight binding site captures the structure in a less reorganized form (Figure 12b, magenta). Nonetheless, the ligand still attempts to relieve strain by uncoiling. The red arrows in Figure 12b illustrate the torquing of the C-2′ C−OH group in response to steric encumbrance. Equally important, the path of the bridge in the New York form runs beneath the baccatin core and is directed toward the deep hydrophobic cleft of the protein. Consequently, this conformation encounters an unfavorable steric contact with Phe272, pushing it further out of the pocket in comparison with the unbridged form (**Figure 12b**). As we have shown previously, a bridge−Phe272 interaction of this type leads to reduced activity for the corresponding taxanes.[38] Accordingly, the New York conformation in complex with tubulin cannot account for the superior activity of the analogues of **5**.

Summary and Conclusions

Important pieces of data in the verification of conformational models of PTX bound to β-tubulin are two intramolecular $^{13}C-^{19}F$ ligand distances determined by double REDOR solid-state NMR.[8] The separations of 9.8 and 10.3 Å, initially associated with an uncertainty of ±0.5 Å, are characterized by several noteworthy features because they pertain to PTX conformation. First, the corresponding T-Taxol conformer values differ by 0.7 and 0.4 Å, respectively, the first difference falling outside the original error estimate by 0.2 Å. One interpretation of the discrepancy can be traced to two torsions in the C-13 side chain. Alteration of both by a diminutive 6° restores perfect agreement with the measurement. Second, a reconsideration of the signal-to-noise in the $\Delta S/S_0$ ratio yields a 6.7% uncertainty in the distances leading to a value of ±0.7 Å rather than an error value of ±0.5 Å. This places the published distances of both T-Taxol and the polar PTX conformation within the expanded error boundaries. Third, in view of the fact that data analysis of the resource-expensive REDOR experiment relied on a single measurement the ±0.7 Å window would appear to be too conservative.

Of equal importance is the fact that the solid-state measurements monitor intramolecular atomic separations deep within the molecular volume of bound PTX. Conformational searches show that the REDOR distances can be maintained by a variety of conformations with a wide spatial dispersion of the C-3′ phenyl rings (Figure 3), which are groups that are in contact with the protein side chains when the molecule is bound. A better measure of the overall shape of the bioactive conformation of PTX would seem to be the distances between the centroids of the terminal *C*-2 and *C*-3′ aromatic rings (Figure 2). On the basis of this criterion, active taxoids **1**, **6**, and **8**, all fit the T-Taxol model, whereas the polar conformation is ruled out in agreement with the inactivity of a set of constrained analogues that mimic it.[7]

The T-Taxol model should not be regarded as a structure characterized by an immutable set of intramolecular distance relationships. Molecular dynamics suggests the presence of a distribution of forms near room temperature (Figure 5b), a distribution that cannot be determined from the single-point REDOR measurement portrayed in Figures 6 and 7. Although the taxane binding site is reasonably well defined, it nonetheless accommodates certain small variations in the placement of the ligand's hydrophobic groups at the molecular periphery. Thus, variations in the location of C-3′ phenyl rings along the wall of the taxane binding pocked are tolerated for both super active and moderately active bridged PTX analogues (e.g., **6** and **8**, respectively) in comparison with PTX (Figures 9 and 10). These observations are also consistent with the proposal that the biological properties of DTX (**2**) and NTX (**4**) are readily accommodated by the T-conformation (Figure 8).

In this work, we have shown that the T-Taxol binding model is as compatible with REDOR-derived intramolecular distances as it is with PTX SAR, photoaffinity labeling results, and acquired mutation-resistance profiles.[10] Crucially, the model has led to the design and synthesis of bridged PTX analogues that match and surpass the bioactivity of paclitaxel itself.[36,39] Equally supportive, the T-Taxol−tubulin model is able to rationalize the capacity of epothilones A and B to assemble and stabilize purified yeast microtubules (*Saccharomyces cerevisiae*) in contrast with PTX's inability to do so.[46] In a follow-up study by the Himes group, the same model provided guidance for the mutation of five yeast tubulin binding-site residues that restored paclitaxel's tubulin assembly activity.[47]

Although the structure of the T-Taxol−tubulin complex employed for analogue designs was derived from electron crystallography (EC) with Zn^{2+} and paclitaxel stabilized sheets,[10,11] the telltale bioassays were performed with genuine microtubules, dispelling the notion that the binding pockets in polymerized tubulin in the two polymeric forms are fundamentally different. Furthermore, as it pertains to the bioactive taxane conformation, we stress that proposals for alternative models (conformations and binding modes) strive, at a minimum, be consistent with the array of data encompassing biophysical measures (the EC density and REDOR distances), biological outcomes (SAR, radiolabeling, and resistant mutants), and the constraints imposed by super-active bridged analogues (e.g. **6**).

Methods

Conformational Searches. Two 15 000-step low mode Monte Carlo conformational searches[16] using MMFF and MM3* force fields and an aqueous continuum solvation model[17] were performed for 2-(*p*-fluorobenzoyl)paclitaxel (**3**) using MacroModel version 8.6.[48] The F−C-5′ and F−C-3′ distances were constrained to the

REDOR values (9.8 and 10.3 Å, respectively).[8] An energy cutoff of 7.0 kcal/mol was used. The search provided 602 and 598 fully optimized MMFF and MM3* conformations, respectively. Distance constraints were removed, and the two sets of conformations were fully optimized in their respective force fields. This resulted in 47 and 33 structures from MMFF and MM3*, respectively, that matched both REDOR distances within ±0.3 Å.

A 10 000 step low mode Monte Carlo conformational search using the MMFF force field in MacroModel and a cutoff of 10.0 kcal/mol was performed for bridged T-Taxol analogue **6** (C-2 *para*-X = H). A total of 93 optimized conformations was obtained, and the global minimum was found 62 times. Twelve of these structures fall into the T-Taxol family on basis of the observation that the centroids of the C-3′ phenyl rings fit the T-form within 20% of the distances found for the centroids of the corresponding T-Taxol phenyl rings, that is, the ranges for the 12 conformers: C-2 benzoyl to benzamide phenyl, 7.9−11.2 Å (T-Taxol 9.4 Å[10]); C-2 benzoyl to C-3′ phenyl, 8.9−9.4 Å (T-Taxol 10.0 Å[10]). Not a single example of the New York conformation PTX-NY was located among the conformers of the optimized dataset.

Finally, a 5000 step low mode Monte Carlo conformational search with an energy cutoff of 7.0 kcal/mol was performed for New York construct **8** using the MMFF94s force field in MacroModel. A total of 105 optimized conformations was obtained, 28 of which conform to the T-Taxol conformation. The global minimum was located 40 times. Again, no conformations corresponded to the New York variation. A single MMFF94s conformer showed a C-13 side chain orientation similar to that in the latter (Figures 11 and 12) and C-3′ phenyl centroid distances within 20% of the T-form (as that above). However, the torsion angles around C-2′ directed the C-2′ OH away from the bridge and, therefore, away from His227 as well when the molecule docked into the protein. This observation is consistent with the behavior of unbridged PTX-NY when subjected to MD within the taxane binding pocket; see the following section.

Molecular Dynamics. The PTX−tubulin complex[10] was subjected to molecular dynamics for 5 ps at 300 K using the Tripos force field in Sybyl version 7.0.[49] The imidazole ring of His227 was treated both in the neutral and protonated states during the separate simulations.

Docetaxel (DTX, **2**) and nonataxel (NTX, **4**) were modified from T-Taxol and docked into the PTX−tubulin complex by superimposing the baccatin cores using Sybyl version 7.0. Each model was subjected to molecular dynamics at 20 K for 5 ps with the protein backbone held as a fixed aggregate. During this treatment, the energy gradually fell until it leveled off during the final picosecond. Because the DTX and NTX complexes were so similar to the starting PTX complex, no further MD was warranted. With the backbone still held fixed, the ligand and the tubulin side chains were then optimized with the Tripos force field.

2-FB-PT was arranged in the PTX-NY conformation with MacroModel version 6.5 by using the C-13 side chain dihedral angles provided by Figure 5 in ref 13b (Figures 11 and 12). This molecule was then manually docked into the 1JFF protein binding site. Molecular dynamics simulations were performed with the MMFF94 force field in Sybyl version 7.0 by allowing movement of the ligand and all of the side chains surrounding it within a 10 Å sphere at 20 K with a time step of 0.5 fs and a dielectric constant of 4.5 for 5 ps. Three constraints were enforced to maintain the PTX-NY conformation throughout the MD simulations: d_1 (F−C(O)) = 10.0 ± 0.2; d_2 (F−C3′) = 9.4 ± 0.2; and C2′-OH−His227-N = 2.5−3.5 Å. The model was regarded as stable because the last 3 ps of the simulation resulted in an overall RMS deviation of 0.35 Å for the ligand and an energy variation of less than 3 kcal/mol. At this point, the constraints were removed, and a full optimization of the site was performed using MMFF94s. The optimized complex was then subjected to higher-temperature MD to determine if the hydrogen bond distance would be maintained without the constraints. The same parameters were used, but the temperature was increased from 20 to 300 K during a 4 ps MD run.

As the molecular dynamic simulations proceeded, the binding pocket of tubulin expanded slightly to better accommodate the ligand, though the only significant change was the position of the His227 side chain. The unprotonated N in the imidazole ring attempted to form a hydrogen bond with the C2′-OH of the ligand (∼3.3 Å). When the constraints were released and the model allowed to follow a dynamic pathway at slightly higher temperatures, the electrostatic interaction between the C2′-OH and His227 was not maintained. Although the ligand stayed within the pocket for the most part, the C-13 side chain, especially the Ph rings, slowly drifted outward and started to lose the PTX-NY conformation (Supporting Information).

REDOR Dephasing Calculations. The REDOR curves were calculated using the formula by Mueller.[50] For the REDOR curves with distance distributions, individual REDOR curves were calculated every 0.1 Å. These curves were summed together and weighted according to a Gaussian distribution.

α,β-Tubulin−Taxol EC Density Maps. The superposition of T-Taxol and PTX-NY was derived from that depicted in Figure 3A of Ojima et al.[13b] The 2Fo−Fc and Fo−Fc electron density maps were generated with CNS 1.1[51] using the 1JFF tubulin−taxol structure and the corresponding structure factors.[11] Taxol parameters and topology were obtained by employing the University of Uppsala's HIC-UP server, v. 9.1−18.[52] For aesthetic purposes, a solvent mask was applied to the resulting 2Fo−Fc electron density map for all densities over 1.5 Å from the protein and the ligands. The analysis and the images were obtained using the programs O, v. 9.0.7[53] and Pymol, v. 0.98.[54]

Acknowledgment. A.A. and J.P.S. are grateful to Dennis Liotta (Emory University), and A.K.M. is appreciative of David Lynn (Emory University) for encouragement and support. We thank James H. Nettles (Emory University) for his advice during the construction of the maps of Figures 11 and 12.

Supporting Information Available: The $2F_{obs}-F_{calc}$ density map and difference maps ($F_{obs}-F_{calc}$) for the 2-FB-PTX-NY−tubulin complex binding site subjected to low-temperature MD simulation and optimization and the coordinates of the EC-refined β-tubulin−PTX structure described in ref 10. This material is available free of charge via the Internet at http://pubs.acs.org.

References

(1) *Taxane Anticancer Agents;* Georg, G. I.; Chen, T. T.; Ojima, I.; Vyas, D. M., Eds.; American Chemical Society: Washington, DC, 1995.
(2) Mekhail, T.; Markman, M. Paclitaxel in cancer therapy. *Expert. Opin. Pharmacother.* **2002**, *3*, 755−766.
(3) Nogales, E.; Wolf, S. G.; Downing, K. H. Structure of the αβ tubulin dimer by electron crystallography. *Nature* **1998**, *39*, 199−203.
(4) Protein data bank (www.rcsb.org/pdb/); pdb 1TUB.
(5) Guéritte-Voegelein, F.; Guénard, D.; Mangatal, L.; Potier, P.; Guilhem, J.; Césario, M.; Pascard, C. Structure of a synthetic Taxol precursor: *N-tert*-butoxycarbonyl-10-deacetyl-*N*-debenzoyltaxol. *Acta Crystallogr., Sect. C* **1990**, *46*, 781−784.
(6) (a) Boge, T. C.; Wu, Z.-J.; Himes, R. H.; Vander Velde, D. G.; Georg, G. I. Conformationally restricted paclitaxel analogues: macrocyclic mimics of the "hydrophobic collapse" conformation. *Bioorg. Med. Chem. Lett.* **1999**, *9*, 3047−3052; (b) Ojima, I.; Chakravarty, S.; Inoue, T.; Lin, S.; He, L.; Horwitz, S. B.; Kuduk, S. C.; Danishefsky, S. J. A common pharmacophore for cytotoxic natural products that stabilize microtubules. *Proc. Natl. Acad. Sci. U.S.A.* **1999**, *96*, 4256−4261; (c) Ojima, I.; Lin, S.; Inoue, T.; Miller, M. L.; Borella, C. P.; Geng, X.; Walsh, J. J. Macrocycle formation by ring-closing metathesis. Application to the syntheses of novel macrocyclic taxoids. *J. Am. Chem. Soc.* **2000**, *122*, 5343−5353; (d) Geng, X.; Miller, M. L.; Lin, S.; Ojima, I. Synthesis of novel C2−C3′ N-linked macrocyclic taxoids by means of regioselective heck macrocyclization. *Org. Lett.* **2003**, *5*, 3733−3736; (e) Querolle, O.; Dubois, J.; Thoret, S.; Dupont, C.; Guéritte, F.; Guénard, D. Synthesis of novel C-2,C-3′N−linked macrocyclic taxoids with variable ring size. *Eur. J. Org. Chem.* **2003**, 542−550; (f) Querolle, O.; Dubois, J.; Thoret, S.; Roussi, F.; Montiel-Smith, S.; Gueritte, F.; Guénard, D. Synthesis of novel macrocyclic docetaxel analogues. Influence of their macrocyclic ring size on tubulin activity. *J. Med. Chem.* **2003**, *46*, 3623−3630.

(7) For a full review of approaches to developing efficacious bridged taxanes see Kingston, D. G. I.; Bane, S.; Snyder, J. P. The Taxol pharmacophore and the T-Taxol bridging principle. *Cell Cycle* **2005**, *4*, 279−289.

(8) Li, Y.; Poliks, B.; Cegelski, L.; Poliks, M.; Gryczynski, Z.; Piszczek, G.; Jagtap, P. G.; Studelska, D. R.; Kingston, D. G. I.; Schaefer, J.; Bane, S. Conformation of mictrotubule-bound paclitaxel determined by fluorescense spectroscopy and REDOR NMR. *Biochemistry* **2000**, *39*, 281−291.

(9) Mastropaolo, D.; Cammerman, A.; Luo, Y.; Brayer, G. D.; Cammerman, N. Crystal and molecular structure of paclitaxel (Taxol). *Proc. Natl. Acad. Sci. U.S.A.* **1995**, *92*, 6920−6924.

(10) Snyder, J. P.; Nettles, J. H.; Cornett, B.; Downing, K. H.; Nogales, E. The binding conformation of Taxol in β-tubulin: A model based on electron crystallographic density. *Proc. Natl. Acad. Sci. U.S.A.* **2001**, *98*, 5312−5316.

(11) Lowe, J.; Li, H.; Downing, K. H.; Nogales, E. Refined structure of $\alpha\beta$-tubulin at 3.5 Å resolution. *J. Mol. Biol.* **2001**, *313*, 1045−1057.

(12) Ivery, T. G. M.; Le, T. Modeling the interaction of paclitaxel with β-tubulin. *Oncol. Res.* **2003**, *14*, 1−19.

(13) (a) Sun, L.; Geney, R.; Xia, S.; Horwitz, S. B.; Pera, P.; Bernacki, R. J.; Ojima, I. *Abstracts of rational design, synthesis and evaluation of conformationally restrained novel paclitaxel analogs*, National Meeting of the American Chemical Society, Philadelphia, PA, Aug 2004; American Chemical Society: Washington, DC, 2004; MEDI-97; (b) Geney, R.; Sun, L.; Pera, P.; Bernacki, R. J.; Xia, S.; Horwitz, S. B.; Simmerling, C. L.; Ojima, I. Use of the tubulin bound paclitaxel conformation for structure-based rational drug design. *Chem. Biol.* **2005**, *12*, 339−348.

(14) Both ref 13 citations reported that "...T-Taxol does not comply with the REDOR-NMR distances with values of 8.11 Å and 9.32 Å..." Unfortunately, as was the case in ref 12, the distances were taken from 1JFF[11] and not from the T-Taxol work[10]; cf. Figure 1.

(15) To clarify conformer identification and terms, the reader should note that the modified T-Taxol conformer proposed by Geney, Ojima, and colleagues was named REDOR-Taxol.[13] As we show in the text, there are nearly 100 PTX conformations that meet the REDOR constraints including T-Taxol. Consequently, we refer to the Geney−Ojima model as New York-Taxol (NY-Taxol).

(16) Kolossváry, I.; Guida, W. C. Low mode search. An efficient, automated computational method for conformational analysis: Application to cyclic and acyclic alkanes and cyclic peptides. *J. Am. Chem. Soc.* **1996**, *118*, 5011−5019.

(17) (a) Still, W. C.; Tempczyk, A.; Hawley, R. C.; Hendrickson, T. Semianalytical treatment of solvation for molecular mechanics and dynamics. *J. Am. Chem. Soc.* **1990**, *112*, 6127−6129; (b) http://www.schrodinger.com/Products/macromodel.html.

(18) Although the coordinates from the original PTX X-ray structure have never been deposited, the paper provides enough information to permit reconstruction.

(19) Cornell, W. D.; Cieplak, P.; Bayly, C. I.; Gould, I. R.; Merz, K. M.; Ferguson, D. M.; Spellmeyer, D. C.; Fox, T.; Caldwell, J. W.; Kollman, P. A. A second generation force field for the simulation of proteins, nucleic acids, and organic molecules. *J. Am. Chem. Soc.* **1995**, *117*, 5179−5197.

(20) Clark, M.; Cramer III, R. D.; Van Opdenbosch, N. Validation of the general purpose Tripos 5.2 force field. *J. Comput. Chem.* **1989**, *10*, 982−1012.

(21) Harper, J. K.; Facelli, J. C.; Barich, D. H.; McGeorge, G.; Mulgrew, A. E.; Grant, D. M. ^{13}C NMR investigation of solid-state polymorphism in 10-deacetyl baccatin III. *J. Am. Chem. Soc.* **2002**, *124*, 10589−10595.

(22) Hing, A. W.; Schaefer, J. Two-dimensional rotational-echo double resonance of Val1-[1-^{13}C]Gly2-[^{15}N]Ala3-gramicidin A in multilamellar dimyristoylphosphatidylcholine dispersions. *Biochemistry* **1993**, *32*, 7593−7604.

(23) Long, H. W.; Tycko, R. Biopolymer conformational distributions from solid-state NMR: α-Helix and 3_{10}-helix contents of a helical peptide. *J. Am. Chem. Soc.* **1998**, *120*, 7039−7048.

(24) Anderson, J. E.; Casarini, D.; Lunazzi, L.; Mazzanti, A. Conformational studies by dynamic NMR. 71.1 Stereodynamics of triisopropyl(aryl)silanes in solution and in the solid state. *J. Org. Chem.* **2000**, *65*, 1729−1737.

(25) Kamihira, M.; Naito, A.; Nishimura, K.; Tuzi, S.; Saito, H. High-resolution solid-state ^{13}C and ^{15}N NMR study on crystalline Leu- and Met-enkephalins: Distinction of polymorphs, backbone dynamics, and local conformational rearrangements induced by dehydration or freezing of motions of bound solvent molecules. *J. Phys. Chem. B* **1998**, *102*, 2826−2834.

(26) Arshava, B.; Breslav, M.; Antohi, O.; Stark, R. E.; Garbow, J. R.; Becker, J. M.; Naider, F. Long-distance rotational echo double resonance measurements for the determination of secondary structure and conformational heterogeneity in peptides. *Solid-State NMR Spectrosc.* **1999**, *14*, 117−136.

(27) Nogales, E.; Whittaker, M.; Milligan, R. A.; Downing, K. H. High-resolution model of the microtubule. *Cell* **1999**, *96*, 79−88.

(28) Diaz, J. F.; Strobe, R.; Engeborghs, Y.; Souto, A. A.; Andreu, J. M. Molecular recognition of Taxol by microtubules. *J. Biol. Chem.* **2000**, *275*, 26265−26276.

(29) Epothilone A, residing in the same pocket, is thought to ride on a small pool of water between the ligand and the protein.[30]

(30) Nettles, J. H.; Li, H.; Cornett, B.; Krahn, J. M.; Snyder, J. P.; Downing, K. H. Mode of epothilone A on α,β-tubulin by electron crystallography. *Science* **2004**, *305*, 866−869.

(31) Igumenova, T. I.; McDermott, A. E.; Zilm, K. W., Martin, R. W., Paulson, E. K. and Wand, A. J. Assignments of carbon NMR resonances for microcrystalline ubiquitin. *J. Am. Chem. Soc.* **2004**, *126*, 6720−6727.

(32) Guéritte-Voegelein, F.; Guénard, D.; Lavelle, F.; Le Goff, M.-T.; Mangatal, L.; Potier, P. Relationships between the structure of Taxol analogues and their antimitotic activity. *J. Med. Chem.* **1991**, *34*, 992−998.

(33) Ojima, I.; Kuduk, S. D.; Pera, P.; Veith, J. M.; Bernacki, R. J. Synthesis and structure−activity relationships of nonaromatic taxoids: Effects of alkyl and alkenyl ester groups on cytotoxicity. *J. Med. Chem.* **1997**, *40*, 279−285.

(34) At one point, a collapsed form of nonataxel served as a template[6b] for the much touted and now abandoned common pharmacophore.[13,30]

(35) Hari, M.; Loganzo, F.; Annable, T.; Tan, X.; Musto, S.; Morilla, D. B.; Nettles, J. H.; Snyder, J. P.; Greenberger, L. M. Paclitaxel resistant cells have a mutation in the paclitaxel-binding region of β-tubulin (Asp26Glu) and less stable microtubules. *Mol. Cancer Ther.* **2006**, *5*, 270−278.

(36) Ganesh, T.; Guza, R. C.; Bane, S.; Ravindra, R.; Shanker, N.; Lakdawala, A. S.; Snyder, J. P.; Kingston, D. G. I. The bioactive Taxol conformation on β-tubulin: Experimental evidence from highly active constrained analogues. *Proc. Natl. Acad. Sci. U.S.A.* **2004**, *101*, 10006−10011.

(37) (a) Halgren, T. A.; Nachbar, R. B. Merck molecular force field. IV. Conformational energies and geometries for MMFF94. *J. Comput. Chem.* **1996**, *17*, 587−615; (b) Halgren, T. A. MMFF VII. Characterization of MMFF94, MMFF94s, and other widely available force fields for conformational energies and for intermolecular-interaction energies and geometries. *J. Comput. Chem.* **1999**, *20*, 730−748; (c) http://www.schrodinger.com/Products/macromodel.html.

(38) Metaferia, B. B.; Hoch, J.; Glass, T. E.; Bane, S. L.; Chatterjee, S. K.; Snyder, J. P.; Lakdawala, A.; Cornett, B.; Kingston, D. G. I. Synthesis and biological evaluation of novel macrocyclic paclitaxel analogues. *Org. Lett.* **2000**, *3*, 2461−2464.

(39) Querolle, O.; Dubois, J.; Thoret, S.; Roussi, F.; Guéritte, F.; Guénard, D. Synthesis of C2-C3′ N-linked macrocyclic taxoids. Novel docetaxel analogues with high tubulin activity. *J.* Med. Chem. **2004**, *47*, 5937−5944.

(40) Rao, S.; He, L.; Chakravarty, S.; Ojima, I.; Orr, G. A.; Horwitz, S. B. Characterization of the Taxol binding site on the microtubule. *J. Biol. Chem.* **1999**, *274*, 37990−37994.

(41) One puzzling feature of the Philadelphia ACS presentation[13] is that the F−C distances for **3** were pictured as F−C2′ and F−C3′ instead of F−C(O) and F−C3′. We presume that the appropriate latter separations were used for the Sun−Ojima measurements of Figure 1.

(42) Sun, L.; Geney, R.; Li, Y.; Ma, K.; Ojima, I. *Abstracts of design, synthesis and evaluation of novel macrocyclic paclitaxel analogues and a de novo paclitaxel mimic*, National Meeting of the American Chemical Society, Washington, DC, Aug, 2005; American Chemical Society: Washington, DC, 2005; MEDI 354.

(43) Alcaraz, A. A.; Snyder, J. P. Unpublished work.

(44) (a) Rhodes, G. *Crystallography made crystal clear: A guide for users of macromolecular models;* Academic Press: San Diego, CA 2000; pp 151−153; (b) McRee, D. *Practical protein crystallography;* Academic Press: San Diego, CA 1999.

(45) Johnson, S. A.; Alcaraz, A. A.; Snyder, J. P. T-Taxol and the electron crystallographic density in β-tubulin. *Org. Lett.* **2005**, *7*, 5549−5552.

(46) Bode, C. J.; Gupta, M. L., Jr.; Reiff, E. A.; Suprenant, K. A.; Georg, G. I.; Himes, R. H. Epothilone and paclitaxel: Unexpected differences in promoting the assembly and stabilization of yeast microtubules. *Biochemistry* **2002**, *41*, 3870−3874.

(47) Gupta, M. L.; Bode, C. J.; Georg, G. I.; Himes, R. H. Understanding tubulin-taxol interactions: Mutations that impart Taxol binding to yeast tubulin. *Proc. Natl. Acad. Sci. U.S.A.* **2003**, *100*, 6394−6397.

(48) Mohamadi, F.; Richards, N. G. J.; Guida, W. C.; Liscamp, R.; Lipton, M.; Caufield, C.; Chang, G.; Hendrickson, T.; Still, W. C. MacroModel − an integrated software system for modeling organic and bioorganic molecules using molecular mechanics. *J. Comput. Chem.* **1990**, *11*, 440−467.
(49) SYBYL: http://www.tripos.com/sciTech/inSilicoDisc/moleculeModeling/sybyl.html; http://uwmml.pharmacy.wisc.edu/SYBYL_user.html.
(50) Mueller, K. T. Analytic solutions for the time evolution of dipolar-dephasing NMR signals. *J. Magn. Reson., Ser. A* **1995**, *113*, 81−93.
(51) Brünger, A. T.; Adams, P. D.; Clore, G. M.; DeLano, W. L.; Gros, P.; Grosse-Kuntsleve, R. W.; Jiang, J.-S.; Kuszewski, J.; Nilges, M.; Pannu, N. S.; Read, R. J.; Rice, L. M.; Simonson, T.; Warren, G. L. Crystallography & NMR system: A new software suite for macromolecular structure determination. *Acta Crystallogr. D* **1998**, *54*, 905−921.
(52) Kleywegt, G. J.; Jones, T. A. Databases in protein crystallography. *Acta Crystallogr. D* **1998**, *54*, 1119−1131.
(53) Jones, T. A.; Zou, J. Y.; Cowan, S. W.; Kjeldgaard, M. Improved methods for building protein models in electron density maps and the location of errors in these models. *Acta Crystallogr. A* **1991**, *47*, 110−119.
(54) DeLano, W. L. *The PyMOL molecular graphics system;* DeLano Scientific: San Carlos, CA, **2002**.

JM051119R